Environmental Pollution 362 (2024) 125015

Contents lists available at ScienceDirect

Environmental Pollution

journal homepage: www.elsevier.com/locate/envpol

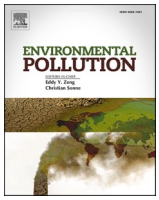

First exploratory study of gaseous pollutants (NO_2, SO_2, O_3, VOCs and carbonyls) in the Luanda metropolitan area by passive monitoring☆

Célia A. Alves [a,*], Manuel J.S. Feliciano [b], Carla Gama [a], Estela Vicente [a], Leonardo Furst [a], Anabela Leitão [c]

[a] Department of Environment and Planning, Centre for Environmental and Marine Studies (CESAM), University of Aveiro, Aveiro, 3810-193, Portugal
[b] Centro de Investigação de Montanha (CIMO), Instituto Politécnico de Bragança, Campus de Santa Apolónia, 5300-253, Bragança, Portugal
[c] LESRA - Laboratório de Engenharia da Separação, Reação e Ambiente, Universidade Agostinho Neto, Av. Ho Chi Minh n° 201, Luanda, Angola

ARTICLE INFO

Keywords:
Luanda
Air quality
Passive sampling
Gaseous pollutants

ABSTRACT

An air quality monitoring campaign for gaseous pollutants using passive sampling techniques was carried out, for the first time, at 25 locations in the metropolitan area of Luanda, Angola, in June 2023. Concentrations of benzene, toluene, ethylbenzene, xylenes, trimethylbenzenes, SO_2 and NO_2 were generally higher in locations more impacted by traffic. Benzene, SO_2 and NO_2 levels did not exceed the World Health Organisation guidelines. Ozone concentrations surpassed those documented for other African regions. Higher O_3 formation potential values were recorded at heavy-trafficked roads. The top 5 species with potential for ozone formation were m,p-xylene, toluene, formaldehyde, propionaldehyde and butyraldehyde. The Mulenvos landfill presented a distinctive behaviour with a very low toluene/benzene ratio (0.47), while values close to 5 were obtained at traffic sites. The maximum levels of α-pinene, D-limonene, formaldehyde, acetaldehyde, acetone, acrolein, propionaldehyde, butyraldehyde, benzaldehyde, valeraldehyde, hexaldehyde and crotonaldehyde were recorded at the landfill. The formaldehyde/acetaldehyde ratio ranged from 0.40 at the Mulenvos landfill to 3.0, averaging 1.8, which is a typical value for urban atmospheres. Acetaldehyde/propionaldehyde ratios around 0.4–0.6 were found in locations heavily impacted by traffic, whereas values between 0.7 and 1.2 were observed in green residential areas and in places with more rural characteristics. All hazard quotient (HQ) values were in the range from 1 to 10, indicating moderate risk of developing non-cancer diseases. The exception was the Mulenvos landfill for which a HQ of 11 was obtained (high risk). The cancer risks exceeded the tolerable level of 1×10^{-4}, with special concern for the landfill and sites most impacted by traffic. A mean lifetime cancer risk of 9×10^{-4} was obtained. The cancer risk was mainly due to naphthalene, which accounted, on average, for 94.6% of the total.

1. Introduction

The new World Health Organisation (WHO) Air Quality Guidelines published in 2021 provide clear evidence of the damage that air pollution inflicts on human health, at even lower levels than previously thought. Indoor and outdoor air pollution is responsible for 7 million deaths annually (WHO, 2016). About 88% of those premature deaths occur in low- and middle-income countries. At the end of 2018, the Air Quality Life Index was introduced to measure the potential gain in life expectancy that communities could achieve if they reduce air pollution to meet guidelines (Greenstone and Fan, 2018). If current levels of air pollution persist, this would cost the average person 1.8 years of life. African countries have some of the world's most polluted cities, where bad air quality is the most potent risk factor. However, they are nearly unrepresented in the research on air pollution and health impacts. Satellite data and models are being used to fill the gap in African cities. However, the effectiveness of predictive models may be limited as they require ground-based measurements to be accurate. Remote sensing, used as proxy for air pollution data, also needs to be calibrated with measurements on the ground (Alvarez et al., 2020; Makoni, 2020). Thus, without adequate monitoring of air quality and limiting the causes of pollution, the problem will only get worse considering the expected

☆ This paper has been recommended for acceptance by Prof. Pavlos Kassomenos.

* Corresponding author.
E-mail address: celia.alves@ua.pt (C.A. Alves).

https://doi.org/10.1016/j.envpol.2024.125015
Received 29 July 2024; Received in revised form 29 August 2024; Accepted 22 September 2024
Available online 23 September 2024

population boom. Air pollution causes about 780,000 premature deaths per year in Africa, according to a modelling study by researchers at NASA (Bauer et al., 2019). Children are the most vulnerable population group. Africa has the 2nd largest number of children living in areas where air pollution exceeds WHO limits. It is estimated that 520 million children are at risk in this continent due to air pollution, based on satellite data. Air pollution kills 18 out of every 10,000 children in Africa before they turn five (WHO, 2018). According to an UNICEF report (Rees et al., 2019), between 1990 and 2017, deaths from outdoor air pollution in Africa grew by 60%, making this the main risk factor for the inhabitants of this continent.

Passive samplers allow assessing the spatial distribution of air pollution in a cost-effective manner. Due to their independence from power sources, small size and light weight, and easy handling without the need of extensive training, passive samplers have proven to be the ideal devices for determining baseline concentrations and as a survey tool. Most air quality monitoring studies based on passive sampling in African countries have been carried out in South Africa, covering places or regions such as the Cape Point Global Atmosphere Watch station (Swartz et al., 2020), the Highveld Priority Area (Josipovic et al., 2010; Lourens et al., 2011), the Durban metropolis (Moodley et al., 2011), and rural areas of the North West Province (Ngoasheng et al., 2021). Some gaseous pollutants were also assessed by passive sampling in Greater Cairo, Egypt (Matysik et al., 2010), Ouagadougou, Burkina Faso (Nana et al., 2012), two Ugandan cities (Kirenga et al., 2015), Fogo Island, Cape Verde (Alves et al., 2018), Abidjan, Ivory Coast (Bahino et al., 2018), seven remote sites in West and Central Africa (Adon et al., 2010), Bamako, Mali, and Dakar, Senegal (Adon et al., 2016), and Meknes City, Morocco (El-Ghazi et al., 2023). As is most African countries, Angola does not have an air quality monitoring network and studies carried out so far are very scarce. As far as we know, only a short-term monitoring campaign involving portable monitors of particulate matter, NO_2, SO_2 and CO was performed at two traffic-impacted sites in Luanda (Campos et al., 2021). Due to the lack of available data on air contaminants in Angola, the general aim of this pilot study was the determination of ambient concentrations of inorganic (NO_2, SO_2 and O_3) and organic (20 volatile organic compounds and 15 carbonyls) gaseous pollutants at various locations in the Luanda metropolitan area using passive samplers. It was also intended to indicate possible sources and/or contributing factors, to compare concentrations with internationally established air quality standards, as well as with measurements conducted elsewhere, to estimate the ozone formation potential of organic pollutants, and to assess possible risks for the residents.

2. Methodologies

2.1. Measurement sites

Located on the Atlantic coast of northern Angola, Luanda is the country's largest city and its capital. The metropolitan region of Luanda, also known as Greater Luanda, is home to a population of about 9 million, which the UN estimates will double by 2030, giving it megacity status. Luanda has a subtropical steppe low-latitude semi-arid hot climate (Köppen-Geiger classification: BSh). The climate is influenced by the offshore Benguela current, which contributes to lowering humidity values, despite the city's latitude, making the hotter months considerably more bearable than similar cities in West/Central Africa. The annual mean temperature is 25 °C with an average monthly variation of 6.5 °C. The average temperature of the coldest month (July) is 21.8 °C and that of the warmest month (March) is 28.1 °C. June (the month of the monitoring campaign) is generally a warm to hot month with a minimum of 20.6 °C, a maximum of 26.5 °C and an average temperature of 23.6 °C. Frequent fog and low clouds prevent temperatures from falling at night even during the completely dry months from May to October. Throughout the year, the city experiences an almost complete absence of rainfall. Precipitation amounts to about 387 mm per year, ranging from 0 mm in the driest months (June and July) to 125 mm in the wettest ones (March and April). The rainy season, typically from December to April, depends on a northerly counter current bringing moisture to the city. There are, on average, around 2280 sunshine hours per year, ranging from 150 in September to 230 in May. In June, 205 sunshine hours are recorded.

Radiello® radial diffusive tubes (Sigma-Aldrich, St. Louis, Missouri, USA) were used for passive sampling of NO_2, SO_2, O_3, volatile organic compounds (VOCs) and carbonyls at 25 points (Table 1) distributed across 6 of the 8 municipalities that make up the Luanda metropolitan region (Cacuaco, Cazenga, Viana, Kilamba Kiaxi, Talatona and Luanda). Given the knowledge of the local reality, the selection of sampling points was carried out jointly by the Agostinho Neto University, the Ministry of the Environment, the Luanda Provincial Government and the Luanda Provincial Command of Civil Protection Services. Sampling took place from June 20th to 30th, 2023. June can be considered a representative month of the average weather conditions recorded in Luanda during a

Table 1
Location and main characteristics of the measurement sites in Greater Luanda.

	Latitude, longitude	Description/Characteristics	Code
1	−8.836501, 13.464893	101th Brigade of Tanks at Funda (rural)	FUNDA
2	−8.800026, 13.425572	Cimangola cement plant at Sequele	CEMEN
3	−8.877330, 13.449981	Sequele wastewater treatment plant	WWTP
4	−8.948658, 13.198022	Lar do Patriota urbanisation, Igreja Pentecostal Street (residential area)	PATRI
5	−8.921424, 13.182824	Oscar Ribas University in Talatona	TALAT
6	−8.908130, 13.223458	Nova Vida urbanisation, residential courtyard (residential area)	NVIDA
7	−8.881899, 13.208479	Interprovincial bus terminal, 21 de Janeiro Avenue (heavy traffic)	BUS
8	−8.851836, 13.209275	Samba Road, next to the maternity entrance (traffic)	SAMBA
9	−8.942213, 13.280516	Campus of the Agostinho Neto University in Camama, on the library's pedestrian avenue	UAN-C
10	−9.003611, 13.280231	Kilamba urbanisation, on the terrace of a building (residential area)	KILAM
11	−8.904152, 13.372376	Viana Municipal Police Command (traffic)	VIANA
12	−8.842251, 13.363823	Mulenvos landfill	MULEN
13	−8.783050, 13.294898	Luanda refinery, parking lot	REFIN
14	−8.811061, 13.242879	Road axis next to Intercontinental Hotel in Miramar district, Luanda (traffic)	MIRAM
15	−8.760712, 13.262703	Lighthouse at the tip of Luanda island (traffic)	LIGHTH
16	−8.807688, 13.238640	Faculty of Sciences on the Luanda waterfront (traffic)	FACSCI
17	−8.824592, 13.238037	Sagrada Familia Square (traffic)	SAFAM
18	−8.829600, 13.238362	Comandante Gika Avenue (or the National Radio Avenue), next to Sonangol gas station (traffic)	GIKA
19	−8.826979, 13.242257	Terrace of the Luanda Firefighters training school, 1st of May Square (traffic)	1MAY
20	−8.818669, 13.242090	Rei Katyavala Street, between the avenues of Portugal and Brasil (traffic)	RKATY
21	−8.807956, 13.248356	Companhia de Jesus Street in Miramar district (residential area of villas)	JESUS
22	−8.837740, 13.234873	Ho Chi Min Lane next to the entrance to the Forum Hotel (traffic)	FORUM
23	−8.833071, 13.224668	Prenda Hospital, next to the main entrance (heavy traffic)	PRENDA
24	−8.847038, 13.230982	21 de Janeiro Avenue, at the entrance to the Faculty of Engineering of the Agostinho Neto University (heavy traffic)	21JAN
25	−8.839977, 13.231916	Ho Chi Min Avenue, next to the intersection with Airport Avenue (heavy traffic)	HOCHI

significant part of the year.

2.2. Sampling and analytical techniques

The system for simultaneous sampling of NO_2 and SO_2 contains the chemiadsorbent cartridge code RAD166, consisting of an inert support of microporous material impregnated with moist triethanolamine (TEA). NO_2 and SO_2 are adsorbed by TEA in the form of nitrite and sulphite ions, respectively, which are easily oxidised and determined by ion chromatography. The O_3 sampler integrates the chemiadsorbent cartridge code RAD172, composed of a hollow cylinder of inert microporous material, filled with silica gel coated with 4.4′-dipyridylethylene and closed at one end by a PTFE cap. During exposure, ozonolysis of 4,4′-dipyridylethylene in an acid environment leads to 4-pyridylaldehyde, which is then condensed with 3-methyl-2-benzothiazolinone hydrazone (MBTH) to produce the corresponding yellow coloured azide. The indirect quantification of O_3 is then carried out by spectrophotometry. VOC samplers (code RAD145) contain an adsorbing cartridge made up of a stainless-steel mesh tube filled with graphite carbon (Carbograph 4). After sampling, VOCs are recovered by thermal desorption and analysed by gas chromatography with mass spectrometer detector. The VOCs analysed and respective detection limits (μg m^{-3}) were as follows: 1,1,1-tricloroethane (0.03), 1,2,3-trimethylbenzene (0.03), 1,2,4-trimethylbenzene (0.03), 1,3,5-trimethylbenzene (0.03), 1,4-dichlorobenzene (0.03), 1-methoxy-2-propanol (0.03), 2-butoxyethanol (0.04), 2-methoxyethylacetate, α-pinene (0.11), benzene (0.05), dimethyl disulfide (0.03), ethylbenzene (0.01), isopropyl acetate (0.02), limonene (0.05), m,p-xylene (0.01), n-butyl acetate (0.05), naphthalene (0.06), o-xylene (0.01), tetrachloroethylene (0.03), toluene (0.01), and trichloroethylene (0.02).

NO_2, SO_2, O_3, and VOCs were analysed at the Istituti Clinici Scientifici Maugeri (Pavia, Italy). The detection limits of NO_2, SO_2 and O_3 were 0.9, 0.8 and 2 μg m^{-3}, respectively. The detailed description of the analytical procedures can be downloaded from the Radiello website.

Samplers for carbonyls (code RAD165) consist of a stainless-steel cartridge filled with 2,4-dinitrophenylhydrazine (DNPH) coated Florisil®. The carbonyl-DNPH derivatives were analysed at the University of Aveiro by adding 2 mL of acetonitrile to the glass tube containing the cartridge. The solution was stirred intermittently for 30 min. Then, the cartridges were removed from the solution, which was analysed by high-performance liquid chromatography (HPLC from Shimadzu Prominence, Germany). The HPLC consists of a degasser (model DGU-20ASR), a solvent distributor (model LC-30AD), an automatic sampler (model SIL-30AC), a diode array detector (model SPD-M20A), and an oven (model CTO-20AC) containing an Ascentis C18 SUPELCO column (15 cm × 4.6 mm, 5 μm). The Lab Solutions software was used to carry out data processing and system control. The method followed in this study was adapted from that described by Marchand et al. (2006). The analytical determination started with a gradient, consisting of a blend of 70% mobile phase A (20% acetonitrile, 60% MilliQ water, and 20% tetrahydrofuran) and 30% mobile phase B (made up of 60% acetonitrile and 40% MilliQ water). After 10 min, the gradient shifted from 70% solvent A and 30% solvent B to 100% solvent B and remained so for the next 40 min. The flow rate was set at 0.7 mL min^{-1} throughout the analysis. The injection volume was 10 μL and the column temperature was maintained at 22 °C. The list of carbonyls analysed and their respective detection limits (μg m^{-3}) were as follows: formaldehyde (0.06), acetaldehyde (0.06), acetone (0.06), acrolein (0.2), propionaldehyde (0.1), crotonaldehyde (0.1), butyraldehyde (0.5), benzaldehyde (0.09), isovaleraldehyde (0.4), valeraldehyde (0.4), o-tolualdehyde (0.2), m-tolualdehyde (0.2), p-tolualdehyde (0.2), hexaldehyde (1) and 2,5-dimethylbenzaldehyde (0.4).

2.3. QA/QC procedures

Sampling was performed according to internationally defined standard procedures (e.g., EPA, 2014; Government of British Colombia, 2018). To capture any potential contamination that may have been introduced during storing, handling, and shipment, 3 trip blanks of each tube type were treated in the same way as the samples. In all blanks, the species analysed were always below the detection limits. Quality control samples included duplicate tubes at 3 sampling sites. The relative percent difference between the paired samples, i.e. precision, was less than 6% for all compounds. In the case of SO_2, NO_2, O_3 and carbonyls, analytical measurements were made in duplicate for all extracts or solutions. The differences between determinations were systematically below 2%. For each compound, 6-point calibration curves with $r^2 > 0.99$ were constructed.

2.4. Spatial analysis

To visualise and analyse the spatial distribution of collected air pollution data, Python was used together with the Cartopy library. OpenStreetMap (OSM) data, which provides detailed and up-to-date geographic information, was used as the base map for the spatial analysis. Each sampling site was represented as a point on the map, with the corresponding pollution levels attributed to these points.

A hierarchical cluster analysis technique, based on the Nearest Point Algorithm to calculate the distance between clusters, was used to statistically identify groups of sites with similar relationships between pollutants. For this analysis, the collected air pollution data were first normalised to ensure that the clustering was not biased due to large differences between the concentrations of various pollutants. Python, along with the clustering package from the SciPy library, were employed.

2.5. Meteorological data

Air pollution data was complemented with meteorological information, which is a key factor influencing the chemical and physical transformations that contaminants undergo in the atmosphere. Meteorological reanalysis data was retrieved from ERA5-Land (Muñoz Sabater, 2019), a state-of-the-art atmospheric reanalysis dataset produced by the European Centre for Medium-Range Weather Forecasts (ECMWF). ERA5-Land offers high-resolution (9 km) hourly data for various meteorological parameters.

For this study, hourly data on temperature, wind speed, and wind direction were extracted and analysed to ensure a reliable representation of weather conditions during the campaign. The air temperature at 2 m above the surface was extracted for the spatial domain from 8.7°S to 9.1°S and from 13.1°E to 13.6°E, covering the entire month of June. Wind speed and direction were analysed at a central cell within this domain.

2.6. Ozone formation potential, photochemical reactivities and secondary organic aerosol potential

In the presence of sunlight, the reactions of gaseous organic compounds and NO_x emitted from vehicle exhausts or other sources can form O_3, which poses a threat to human health, crop production and vegetation. The ozone formation potential (OFP) of the compounds monitored in Luanda was calculated as follows (Tan et al., 2012):

$$OPF_i\ (\mu g\ m^{-3}) = MIR_i \times C_i \quad (1)$$

where MIR_i is the maximum incremental reactivity (dimensionless, gram of O_3 produced per gram of carbonyl or other VOC i) and C_i is the concentration (μg m^{-3}) of each compound. In this study, MIR coefficients were taken from Venecek et al. (2018).

Propene-equivalent concentrations (*Prop-Equiv*) have been widely applied to estimate the photochemical reactivity of carbonyls and other VOCs with OH radicals. The Prop-Equiv scale is an OH-reactivity

indicator based on a scale normalised to the reactivity of propene. It is a measure of the concentration of propene needed to generate a carbon oxidation rate equal to that of a specific VOC species:

$$Prop\text{-}Equiv_i = C_i \times k_{OH\ i}/k_{OH\ (propene)} \quad (2)$$

where C_i is the concentration of each carbonyl or VOC, $k_{OH\ i}$ is the rate coefficient of each species i with OH radical and $k_{OH\ (propene)}$ is the rate coefficient of propene with OH radical (26.3×10^{-12} cm^3 $molecule^{-1}$ s^{-1}). The k_{OH} value of each compound was obtained from Atkinson and Arey (2003).

The potential to form secondary organic aerosols (SOAP) was calculated using measured VOC concentrations and the SOAP coefficient of individual VOCs species based on Derwent et al. (2010):

$$SOAP = \sum C_i \times SOAP_i \quad (3)$$

2.7. Health risk assessment

The inhalation health hazard quotient (HQ) was estimated by applying the equation for long-term exposure:

$$HQ_i = C_i/R_fC_i \quad (4)$$

where, C_i is the concentration of each pollutant i in the air (μg m^{-3}), and R_fC_i is the pollutant-specific reference concentration (μg m^{-3}). Human health risks due to inhalation of carcinogens were calculated as follows:

$$Cancer\ risk_i = C_i \times IUR_i \quad (5)$$

where C_i is the ambient air concentration of each pollutant (μg m^{-3}), and IUR_i is the pollutant-specific inhalation unit risk factor (μg m^{-3}). Table S1 (supplementary material) compiles the R_fC and IUR values used in the present study. The IUR of each pollutant represents the excess lifetime cancer risk as a result of the continuous exposure to that pollutant at a concentration of 1 μg m^{-3} over a lifetime of 70 years. The individual cancer risk of each VOC and carbonyl was assumed to be additive, and thus, the global lifetime cancer risk was estimated as the sum of the cancer risks of the individual compounds.

A semi-quantitative risk assessment was also carried out following the methodology described by Hou et al. (2024). A risk index (R), categorised into 5 classes (1 - negligible risk, 2 - low risk, 3 - moderate risk, 4 - high risk, 5 - very high risk), was calculated:

$$R = \sqrt{HR \times ER} \quad (6)$$

where HR and ER are the hazard and exposure rates, respectively. HR values vary from 1 to 5 depending on the toxicity of each compound and can be found in documents from the American Association of Governmental Industrial Hygienists, the International Agency for Research on Cancer, and other international organisations. The ER can be calculated by dividing the exposure concentrations (E) by the R_fC of each compound, rather than the occupational exposure limits used for indoor air. When $E/R_fC < 0.1$, ER is 1; $0.1 \leq E/R_fC < 0.5$, ER is 2; $0.5 \leq E/R_fC < 1.0$, ER is 3; $1.0 \leq E/R_fC < 2.0$, ER is 4; and $E/R_fC \geq 2.0$, ER is 5. The measured concentrations were taken as representative of the levels to which the population is exposed.

3. Results and discussion

3.1. Meteorological conditions

Temperature data for Luanda in June 2023 are shown in Fig. S1 (Supplementary Material). This figure displays the time series of the domain-averaged values (solid line) and the range of values (shaded area), illustrating the variability within the domain over time. The data show striking diurnal patterns, with daily temperatures exhibiting a mean difference of 8 °C between daily minima and maxima, while maintaining relatively stable values throughout the month.

Wind data for the campaign period are represented as a wind rose diagram (Fig. S2). Winds were primarily from the South-Southwest, South and Southwest sectors, with 50% of the hours with average wind speeds lower than 1.4 m s^{-1}. The maximum hourly average wind speed was 3.3 m s^{-1}.

The time series of wind data during the campaign period revealed variations in wind dynamics. In the first and last days of the sampling campaign, the wind blew mainly from the South quadrant during the night and from the West quadrant during the afternoon. Between June 23 and 27, the wind became more stable, blowing from the South quadrant 95% of the time.

3.2. Concentrations of gaseous pollutants and spatial distribution

Concentrations of all constituents by location can be found in the supplementary material (Table S2). Considering the compounds that systematically presented concentrations above the detection limits, the correlation matrix between sites and the dendrogram were calculated (Fig. 1). Hierarchical clustering clearly revealed that the Mulenvos landfill (MULEN) is different from other sampling places. REFIN and RKATY were identified as similar to each other and different from all other locations. These two sites presented n-butyl acetate concentrations much larger than all other sampling points (Fig. 2). The remaining sites formed a large cluster of sampling points (portrayed in green in Fig. 1) representative of city-wide background concentrations, such as residential and pedestrian areas. This cluster also includes the wastewater treatment plant, which, despite having a different profile, is located in a peripheral site with rural characteristics and low traffic emissions. A second important cluster (represented in orange in Fig. 1) could be identified, containing mostly central locations impacted by road traffic (PRENDA, GIKA, 21JAN, FORUM, MIRAM, FACSCI, VIANA and SAFAM), where greater intensity and stop-and-go driving conditions contribute to higher emissions.

Of the 20 VOCs analysed, some systematically presented very low levels in all samples. These included 1,1,1-trichloroethane (<0.045 μg m^{-3}), 1,4-dichlorobenzene (<0.041 μg m^{-3}), 1-methoxy-2-propanol (<0.089 μg m^{-3}), 2-butoxyethanol (<0.089 μg m^{-3}), 2-methoxyethylacetate (<0.043 μg m^{-3}), dimethyl disulfide (<0.038 μg m^{-3}), and isopropyl acetate (<0.035 μg m^{-3}). The geographical distribution of the most representative VOCs is shown in Fig. 2. Benzene, toluene, ethylbenzene, and xylenes, commonly referred to as BTEX, were the most abundant VOCs. In a review paper, Sekar et al. (2019) compiled the worldwide available air quality standards for benzene and compared its concentrations in outdoor air of different countries. Although the limits imposed vary, most countries have adopted an air quality standard of 5 μg m^{-3} (annual mean). The mean levels documented in the bibliography were 371.4 ± 1567 μg m^{-3}, 5.6 ± 6.6 μg m^{-3}, and 44.6 ± 189.6 μg m^{-3} in Asian, European and North American countries, respectively. BTEX levels in Luanda were lower than those reported for urban areas of some other African countries (Table 2).

Ratios between BTEX species, such as toluene to benzene (T/B), have been used to distinguish contributions from traffic emissions from those from other sources. However, these ratios depend on the composition of the vehicle fleet and the fuels used, as well as the presence of other sources. Zhang et al. (2016) collected source profiles and delimited the relative proportions of benzene, toluene and ethylbenzene in a tertiary plot (Fig. 3). In the present work, the distinctive behaviour of the sample from the Mulenvos landfill stands out, where smouldering combustion of waste is constantly observed. For this location, a very low T/B value (0.47) was obtained compared to the other sampling points. The remaining points fall in the region of the graph corresponding to traffic emissions, although there is overlap with industrial emissions for a subset of samples. This subset was collected in locations most heavily impacted by traffic, generating a T/B of 4.97 ± 0.63, while the other subset (T/B = 2.57 ± 0.65) corresponds to samples from residential

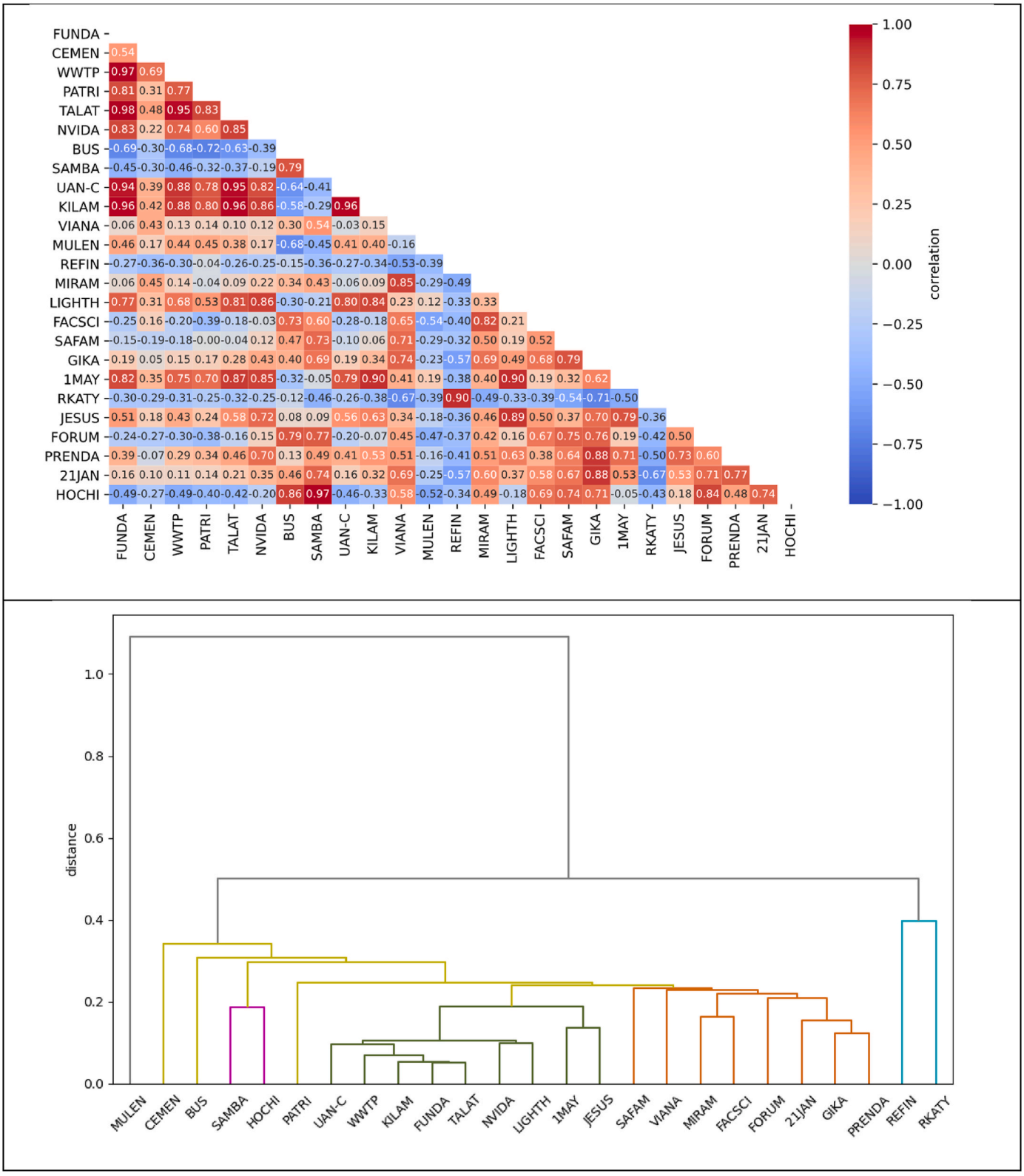

Fig. 1. Correlation matrix and dendrogram for the 25 sampling locations.

areas or further away from busy roads. Thus, it appears that the typical T/B for traffic emissions in Luanda is a value close to 5. Excellent bivariate linear correlations were obtained between BTEX ($r^2 > 0.95$; Table S3, Supplementary Material), pointing to traffic as a common source.

In an assessment of BTEX emissions from gasoline-fuelled private cars in Hong Kong, Guo et al. (2011) concluded that the T/B ratio depends on the driving speed. The highest T/B was registered at 50 km h^{-1}. The authors also argued that toluene can be used as an unleaded gasoline additive to increase the octane number and thus higher T/B ratios can be obtained in regions where this additive is incorporated into the fuel. The Angolan fleet is dominated by gasoline vehicles. Cachon

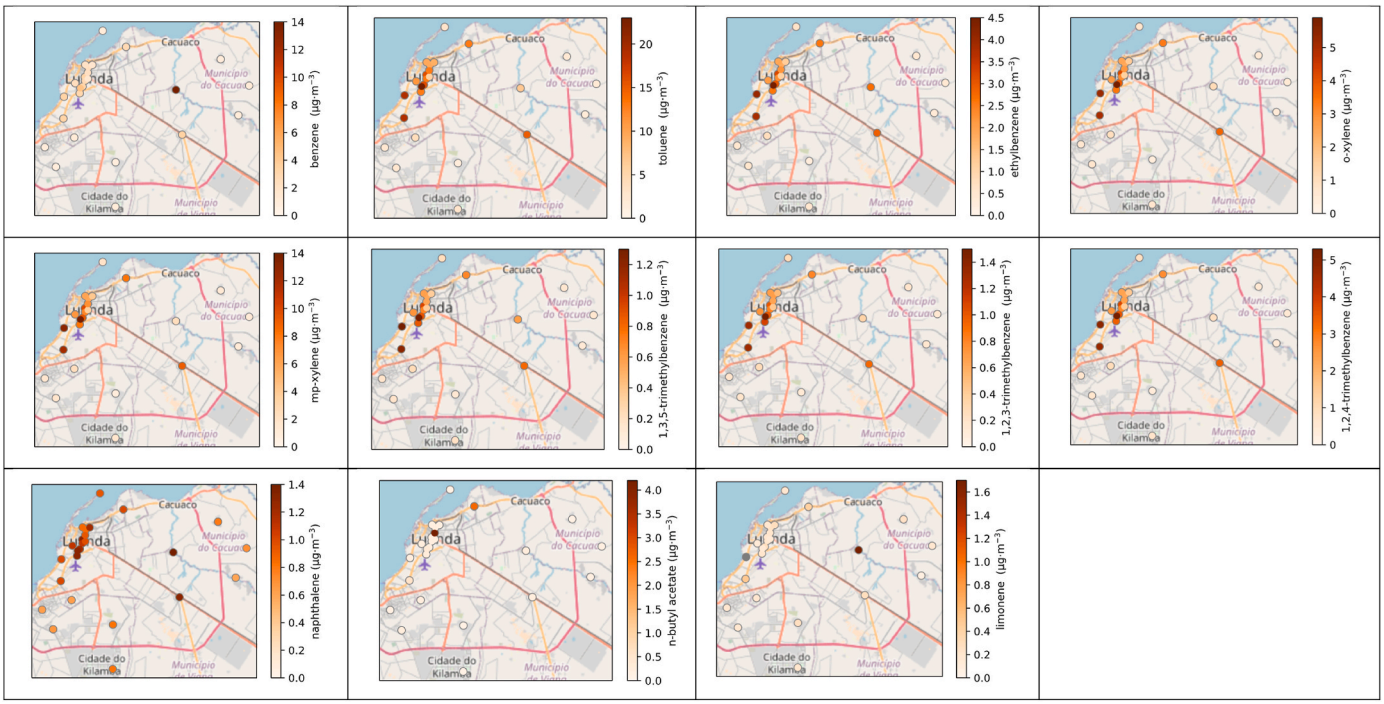

Fig. 2. Geographical distributions of the most abundant VOCs in Greater Luanda. Gray dots represent sampling locations where measurements were below the detection limit.

Table 2
BTEX concentrations (µg m^{-3}) in Luanda and reported in the literature for other African regions.

	Benzene	Toluene	Ethylbenzene	m,p-Xylene	o-Xylene	Reference
Luanda						This study
Roadside (heavy traffic)	2.76 ± 0.77	13.7 ± 4.51	2.61 ± 0.98	8.31 ± 3.03	3.41 ± 1.27	
Residential and other sites	0.95 ± 0.12	2.46 ± 0.78	0.49 ± 0.14	1.54 ± 0.48	0.62 ± 0.19	
Landfill	14	6.6	2.7	2.4	1.1	
S. Filipe, Fogo Island, Cape Verde	1.1	41.8	10.4	8.0	3.0	Alves et al. (2018)
Meknes, Morocco						El-Ghazi et al. (2023)
Urban background	2.04	25.12	3.57	13.98	7.70	
Traffic	1.40	12.50	2.03	7.82	2.57	
Inezgane-Ait Melloul, Morocco						Ouabourrane et al. (2017)
Roadside	4.8 ± 1.2	10.8 ± 1.6		6.6 ± 1.6	3.5 ± 1.3	
Greater Cairo, Egypt	7.81	22.84	3.07	11.57	3.88	Matysik et al. (2010)
Algiers, Algeria						Kerbachi et al. (2006)
Roadside	27.1 ± 11.7	39.2 ± 14.9	6.3 ± 4.3	19.2 ± 8.6	7.6 ± 4.0	
Urban	9.6 ± 4.3	15.2 ± 5.3	0.9	3.2 ± 2.9	Not detected	
Semi-rural	6.5 ± 0.9	13.7 ± 2.6	0.8 ± 0.5	2.8 ± 0.8	Not detected	
Nairobi, Kenya						Cordell et al. (2021)
Urban background	4.95 ± 1.74	5.94 ± 3.86	1.10 ± 0.64	1.66 ± 1.06	1.15 ± 0.72	
Roadside	21.60 ± 7.09	44.5 ± 17.14	8.38 ± 3.25	14.73 ± 5.88	10.72 ± 4.33	
Lagos, Nigeria						
Urban background	4.20 ± 2.20	9.10 ± 3.40	1.84 ± 1.13	4.26 ± 1.71	1.54 ± 0.47	
Roadside	24.23 ± 7.29	32.89 ± 8.27	15.13 ± 6.71	25.01 ± 11.96	8.86 ± 5.08	
Ouagadougou, Burkina Faso						Nana et al. (2012)
Urban background	29.7	68.8	11.6	60.4	9.6	
Roadside	26.2	55.4	11.5	58.0	10.8	
Welgegund, regional background, South Africa						Jaars et al. (2018)
2011–2012	0.93	3.35	1.48	3.34	1.3	
2013–2013	0.35	32.4	8.86	25.2	7.9	

et al. (2013) carried out an analysis of the composition of gasoline obtained from African (Nigeria and Benin) and European fuel stations. The T/B ratio varied between 1.27 and 10.25. The researchers presented a comparison with the ratios reported for gasoline from different countries, mentioning values of 6.59–15.54 for Italy, 1.68 for São Paulo, Brazil, 5.54 for Atlanta, USA, 2.01 for Santiago, Chile, 7.07 for Hong Kong, and more general ratios of 3.33 and 3.56 for Brazil and the USA. Differences between ratios may be due to, among other factors, the benzene content in gasoline. Although the concentration of benzene in fuels sold in the European Union must be less than 1.0% by volume, in many other countries, especially in Africa, the content is still not regulated. In Angola, the benzene content in fuels, around 1%, is lower than that observed in other African countries (Guéniat et al., 2016).

The m,p-xylenes/ethylbenzene (X/E) ratio has been used as an indicator of the photochemical age of an urban plume (Kim et al., 2019). As m,p-xylenes react more rapidly than other compounds, a X/E value significantly below 3 suggests a greater likelihood of reactions involving xylenes and OH radicals, shorter VOC persistence, and the presence of

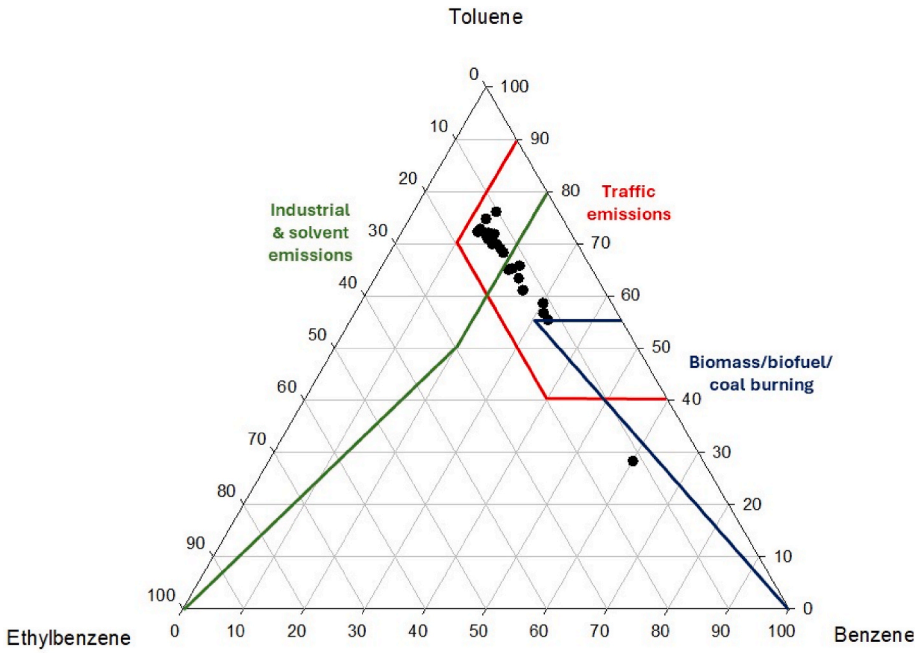

Fig. 3. Relative proportions of benzene, toluene, and ethylbenzene in emission profiles of various sources (Guo et al., 2011), and values of the present study (black dots).

aged air masses. Excluding the value obtained for the Mulenvos landfill (0.88), a relatively constant ratio (3.2 ± 0.14) was obtained in the metropolitan area. The stability of the X/E ratio demonstrates that the intensity of emissions from xylene and ethylbenzene sources greatly exceeds their photochemical removal. Values between 2.81 and 4.6 have been reported for vehicle exhaust emissions, roadside and road tunnel measurements (Monod et al., 2001).

Three trimethylbenzenes (TMBs), which are C9 alkylbenzenes, were detected: 1,2,3-TMB (hemimellitene), 1,2,4-TMB (pseudocumene), and 1,3,5-TMB (mesitylene). TMBs are produced during petroleum refining. Vehicle emissions are also a major anthropogenic source of TMBs, due to the widespread use of the C9 fraction as a component of gasoline. Besides their toxicity to humans, atmospheric oxidation mechanisms of TMBs can play a significant role in the formation of tropospheric ozone and SOA (e.g., Tsiligiannis et al., 2019). The TMB concentrations observed in Greater Luanda were within the values documented for the Pearl River Delta region in China (Zhang et al., 2013) and lower than those in the atmosphere of Karachi, Pakistan, where mean levels of 1.97 μg m^{-3} and 4.92 μg m^{-3} were obtained (Barletta et al., 2002). In the capital of Angola, the highest concentrations of the three structural isomers were attained in the most traffic-congested locations. The excellent intercorrelations between them (Table S3) are a strong indication that road traffic is the main emission source of these VOCs. Investigations on atmospheric TMB concentrations in Africa are very scarce. Cordell et al. (2021) reported mean levels of 3.77, 12.24 and 3.03 μg m^{-3} for hemimellitene, pseudocumene and pseudocumene, respectively, at roadside sites in Nairobi, while the corresponding values for the urban background were 0.38, 1.22 and 0.31 μg m^{-3}. The same authors also provided concentrations for 1,2,3-TMB (2.27 versus 0.18 μg m^{-3}), 1,2,4-TMB (9.17 versus 1.03 μg m^{-3}) and 1,3,5-TMB (2.74 versus 0.26 μg m^{-3}) at roadside and urban background sites in Lagos. The annual median values of 1,2,3-TMB, 1,2,4-TMB and 1,3,5-TMB in Greater Cairo were 1.37, 5.2 and 1.52 μg m^{-3}, respectively (Matysik et al., 2010).

Two monoterpenes from vegetation, α-pinene and D-limonene, were quantified in the passive samples. For most locations in the city centre, α-pinene concentrations were below 0.12 μg m^{-3}. In more vegetated areas, levels fell within a narrow range from 0.12 to 0.14 μg m^{-3}. For most sites, D-limonene concentrations were between approximately 0.2 and 0.3 μg m^{-3}. The maximum levels of α-pinene (0.42 μg m^{-3}) and D-limonene (1.7 μg m^{-3}) were obtained at the Mulenvos landfill. Terpenes such as α-pinene and D-limonene are known to be emitted during the aerobic and anaerobic degradation processes of solid wastes. Furthermore, municipal landfills, along with organic wastes, contain plant debris and household products like cleaning and personal care products, paints, textiles, etc., which also emit large amounts of VOCs (Nair et al., 2019; Pan et al., 2023). It was also at the Mulenvos landfill that the highest concentrations of many carbonyls were recorded, such as formaldehyde, acetaldehyde, acetone, acrolein, propionaldehyde, butyraldehyde, benzaldehyde, valeraldehyde and hexaldehyde. Crotonaldehyde was only detected at the landfill, while isovaleraldehyde, o-tolualdehyde and 2,5-dimethylbenzaldehyde were always absent, regardless of location.

Among carbonyls, the most abundant was butyraldehyde, followed by formaldehyde, propionaldehyde and acetaldehyde (Fig. 4). It is well known that vehicle emissions are major sources of carbonyls. Formaldehyde and acetaldehyde are also produced by photochemical oxidation of hydrocarbons. These two species have been targeted in several toxicological studies owing to their detrimental health effects (e.g., Leikauf, 2020; LoPachin and Gavin, 2014; Tian et al., 2022), and their concentrations have been measured in many urban areas around the world (Delikhoona et al., 2018; Guo et al., 2014; Lü et al., 2010; Wang et al., 2022; and references therein). The concentrations obtained in this study are within the wide range of results reported for other regions. For comparative purposes, the levels of some carbonyls obtained in the few studies carried out in Africa and those in the present study are displayed in Table S4. The concentration ratio of formaldehyde/acetaldehyde (C_1/C_2) has been used to assess the origin of these carbonyls. C_1/C_2 ratios normally range from 1 to 2 in urban atmospheres to about 10 at forested rural areas (Lü et al., 2010). In this study, C_1/C_2 varied from 0.40 at the Mulenvos landfill to 3.0 at the Agostinho Neto University campus in Camana, averaging 1.8. The acetaldehyde/propionaldehyde ratio (C_2/C_3) has also been used as an indicator of the origin of compounds, given that propionaldehyde is mainly associated with anthropogenic emissions, while other carbonyls have both natural and anthropogenic sources. Therefore, C_2/C_3 ratios are higher in rural

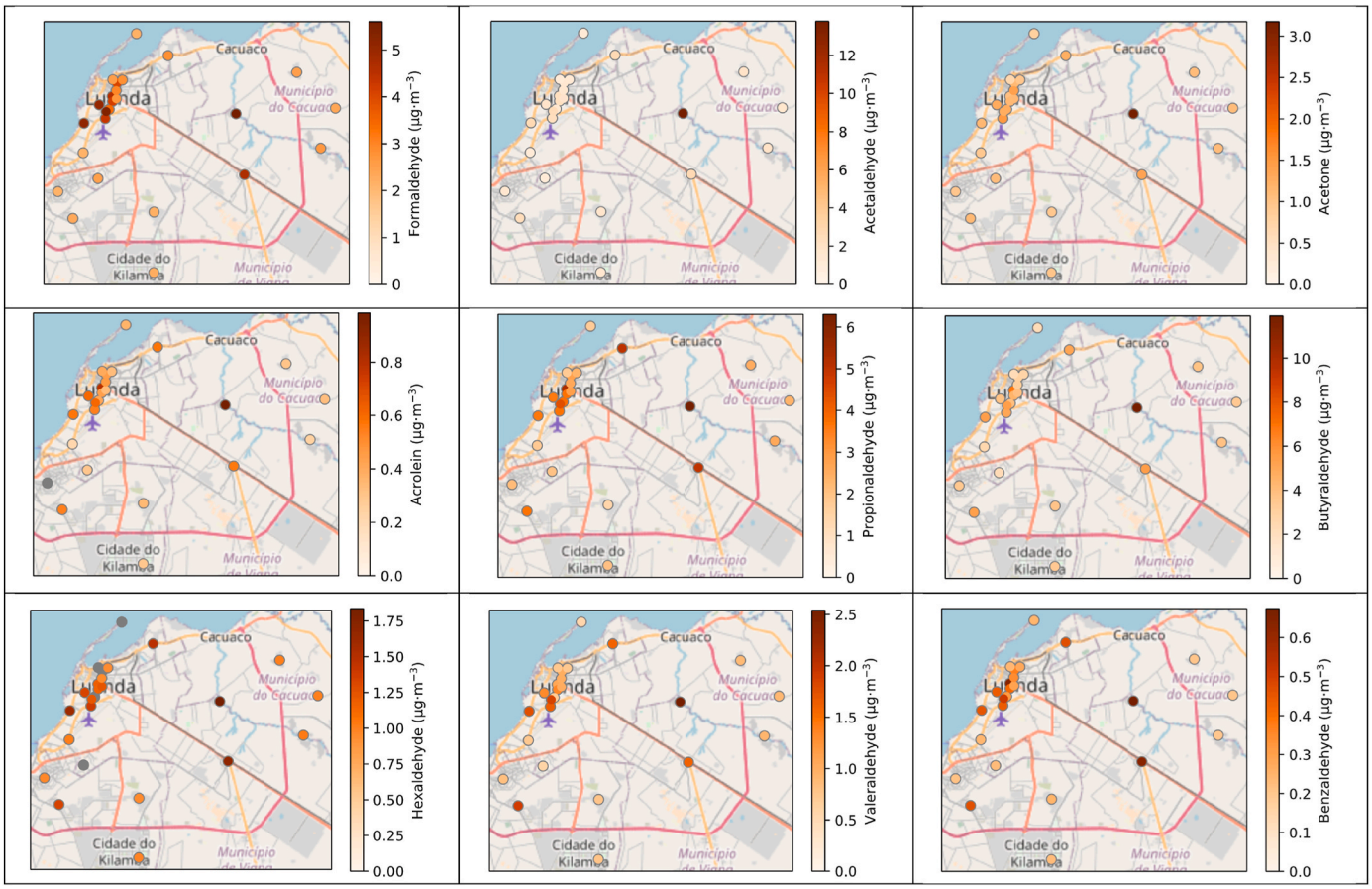

Fig. 4. Geographical distribution of the most abundant carbonyls in Greater Luanda. Gray dots represent sampling locations where measurements were below the detection limit.

atmospheres and lower in polluted urban air. An average ratio of 0.69 was obtained, with values ranging from 0.39 on a very busy avenue to 2.2 at the landfill. Globally, C_2/C_3 values around 0.4–0.6 were found for locations heavily impacted by traffic, whereas ratios between 0.7 and 1.2 were observed in green residential areas and in places with more rural characteristics.

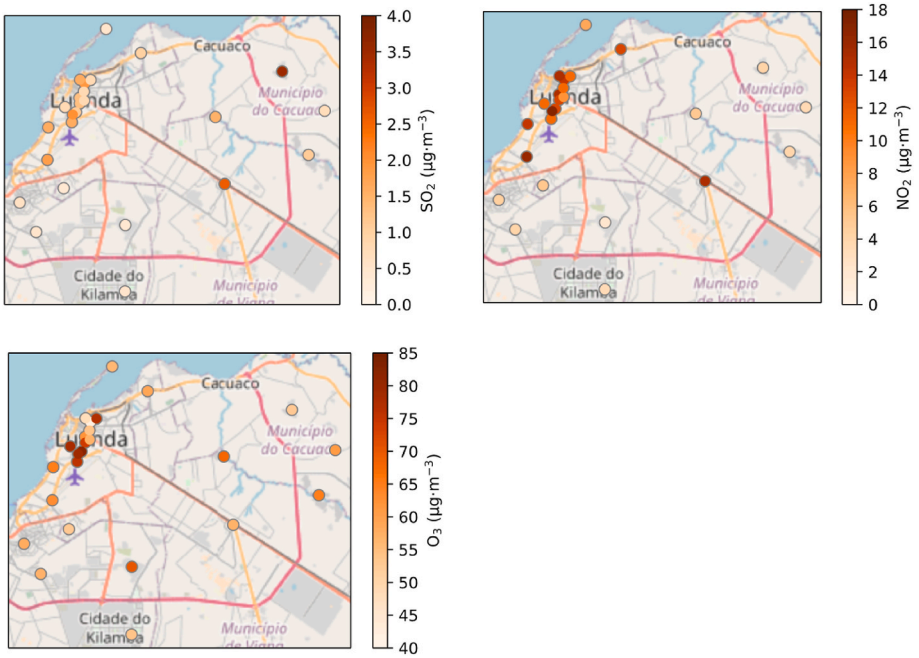

Fig. 5. Geographical distribution of SO_2, NO_2 and O_3 levels in Greater Luanda.

SO_2 concentrations never exceeded 3.5 μg m^{-3} (Fig. 5), well below the daily guideline of 40 μg m^{-3} recommended by the WHO. The maximum value was recorded at the cement factory campus in Sequele. SO_2 emissions in this type of industrial unit are mainly originated from sulphides in the raw meal and limestone. Although SO_2 can be formed from the petroleum refining process, the concentrations of this and other gaseous pollutants in the vicinity of the refinery were relatively low. Plumes emitted by stacks rise into the atmosphere and, thus, gaseous pollutants are expected to be found at a slightly higher altitude. On the other hand, in 2022, an expansion and modernisation project was concluded aimed at increasing fourfold the refinery's gasoline production capacity. As part of this project, the combined cycle was rehabilitated to be fed by hydrogen produced by the new Platforming unit, and power is now generated recycling gas with a net reduction of pollutant emissions. Locations most impacted by traffic had higher concentrations of SO_2 than those with a more rural or residential profile.

NO_2 concentrations ranged from 2.1 μg m^{-3} on the Agostinho Neto University campus to 17 μg m^{-3} on an avenue with very congested traffic that intersects another avenue leading to the airport. The levels obtained did not exceed the daily guideline of 25 μg m^{-3} stipulated by the WHO, although some caution is needed in the comparison because the values of the present study represent an average of 10 days. Bahino et al. (2018) presented an overview of the few urban NO_2 and SO_2 monitoring studies in African cities. NO_2 values varied between 4.7 μg m^{-3} in Amersfoort, South Africa, and 66.8 μg m^{-3} in Cairo, Egypt, while SO_2 ranged from 5.2 μg m^{-3} in Abidjan, Ivory Coast, to 41.6 μg m^{-3} in Dakar, Senegal. Using portable monitors, Campos et al. (2021), in a short-term campaign, measured NO_2 and SO_2 in two avenues, one located in the city centre, and the other one in Talatona, a municipality bordering Luanda, which currently houses several administrative and economic services that were relocated from the central zone of the capital. SO_2 values of 114 μg m^{-3} (weekdays) and 68.2 μg m^{-3} (weekends) were reported for the most central avenue, while the corresponding levels in Talatona were 11.6 and 6.72 μg m^{-3}. NO_2 concentrations were 78.9 μg m^{-3} (weekdays) and 81.2 μg m^{-3} (weekends) in the centre of Luanda and 65.2 μg m^{-3} (weekdays) and 75.8 μg m^{-3} (weekends) in the neighbouring municipality. The higher concentrations reported by Campos et al. (2021) compared to those in the present study may be related to the fact that the previous campaign was carried out in a different season (January–March 2020), covering measurements only during the daytime period (7 a.m. - 10 p.m.).

The average O_3 value was 63 μg m^{-3}, ranging from 42 to 82 μg m^{-3}. O_3 levels recorded in Luanda were higher than those documented for other African regions, such as Abidjan, Ivory Coast (10.0–37.5 μg m^{-3}, Bahino et al., 2018), Dakar, Senegal (15.1 μg m^{-3}, Adon et al., 2016), Bamako, Mali (10.0 μg m^{-3}, Adon et al., 2016), and the highly industrialised area of Mpumalanga Highveld in South Africa (<10–84.4 μg m^{-3}, averaging 38 μg m^{-3}, Josipovic et al., 2010). The WHO guideline values are 100 μg m^{-3} for the 8-h mean and 60 μg m^{-3} for the "peak season" mean. Ozone concentrations are generally lower in urban locations with heavy traffic compared with downwind suburban areas where nitrogen oxide pollution is quite low and thus less O_3 depletion occurs. Paradoxically, in Luanda, higher concentrations were recorded at heavy-trafficked roads and junctions than in more peripheral locations. However, the photochemistry of ozone is a complex and highly non-linear process and, in addition, to the VOC/NO_x ratios, its concentrations depend on several other parameters such as cloud cover, synoptic meteorology, local-scale wind conditions, distribution and strength of emission sources, etc. Liu et al. (2022) observed no significant difference in the O_3 concentration between roadside and urban background environments in Guangzhou, China, arguing that alkoxy radicals (RO) and hydroperoxyl radicals (HO_2) generated by the reaction of VOCs and hydroxyl (OH) radicals in the atmosphere also react with NO, destroying the dynamic balance between NOx and O_3 and increasing the concentration of the latter. Excluding the value of the landfill (7.27), in Luanda, the VOC to NO_2 (VOCs/NO_2, ppbvC/ppbv) ratio was 2.03 ± 0.63. Although this ratio is underestimated because not all VOCs present in the atmosphere were determined, it indicates that the O_3 formation regime in the study sites is VOC-limited, and that VOC emission control is critical to O_3 alleviation. The photochemistry of Luanda's atmosphere deserves to be investigated in future work.

3.3. Ozone formation potential and secondary organic aerosol potential of VOCs

An OFP of 231 ± 113 μg m^{-3} was obtained, varying from 93 to 457 μg m^{-3}, respectively, on the Agostinho Neto University campus in Camana and at the intersection point between two of the busiest avenues in Luanda (Av. Ho Chi Minh and Av. Revolução de Outubro, which gives access to the airport). According to the abundance of precursors, the highest OFP values were found in locations most influenced by traffic, while more residential and peripheral areas showed lower levels. The top 5 ozone formation species were m,p-xylene, toluene, formaldehyde, propionaldehyde and butyraldehyde, which accounted for 15.3, 14.6, 11.6, 10.3 and 12.2% of the total OFP, respectively. If the Muvenvos landfill values are taken as outliers and are not considered, and excellent linear relationship between OFP and Prop-equiv concentrations ($y = 0.10x+2.64$, $r^2 = 0.99$) was obtained, indicating significant correlations between the OH reactivity and ozone formation from VOCs. The total Prop-Equiv concentration was 27 ± 12 μg m^{-3}, ranging between 12 and 51 μg m^{-3}. The largest contributors to Prop-Equiv were butyraldehyde (16.0%), m,p-xylene (13.9%) and propionaldehyde (9.7%).

In Moscow, for all VOCs measured during the summers of 2011–2013, the OFP values did not exceed 115 μg m^{-3} (Berezina et al., 2020). An average OFP of 220 μg m^{-3} was obtained from measurements at 5 five sites in Kaifeng, China (Chen et al., 2023). Tan et al. (2012) reported an OFP of 863 μg m^{-3} and a Prop-Equiv of 260 μg m^{-3} for winter measurements in Foshan, a polluted city also in China. The total OFPs for roadside locations in Nairobi and Lagos were 1055 μg m^{-3} and 1184 μg m^{-3}, respectively, and were higher than their corresponding background sites, by a factor of 5.3 and 4.8 (Cordell et al., 2021). It should be noted, however, that comparisons should be taken as merely indicative because the number and type of compounds determined in the different studies do not coincide.

The average total SOAP of the VOCs analysed was 2199 μg m^{-3}, varying from 411 μg m^{-3}, in a location with characteristics of an urban background atmosphere, to 5171 μg m^{-3} for one of the most congested avenues in the metropolis. These values are in the ranges reported for Chinese megacities (Hui et al., 2018; Li et al., 2020). The top 5 contributing species to the total SOAP were toluene, m,p-xylene, benzene, ethylbenzene and benzaldehyde, accounting for 40.9, 19.4, 12.1, 9.1 and 5.1%, respectively.

3.4. Human health risks

The HQ considers that there is a threshold below which it is unlikely that adverse health effects would occur. If the exposure level exceeds the reference concentration (HQ > 1), adverse non-cancer effects are expected. In general, the following severity scales are used (Thabethe et al., 2014): QH < 1, no hazard; HQ from 0.1 to 1.0, low hazard; HQ from 1.1 to 10, moderate hazard; HQ > 10, high hazard. In Luanda, all values were in the range of 1–10, except at the landfill, where an HQ of 11 was obtained (Fig. 6). At this location, the compounds that contributed most to the HQ were benzene (42.9%), acrolein (25.9%) and acetaldehyde (14.1%). Globally, for all 25 sites, the most significant contributions were those from acrolein (35.8%), benzene (21.6%), propionaldehyde (11.9%), formaldehyde (11.3%), naphthalene (8.3%) and acetaldehyde (7.1%).

To prevent the occurrence of oncological diseases, the USEPA considers that the cancer risk must be above the acceptable level of 1×10^{-6}, but below the tolerable risk of 1×10^{-4} (Zhang et al., 2021; and references therein). In Luanda, all values exceeded the tolerable limit,

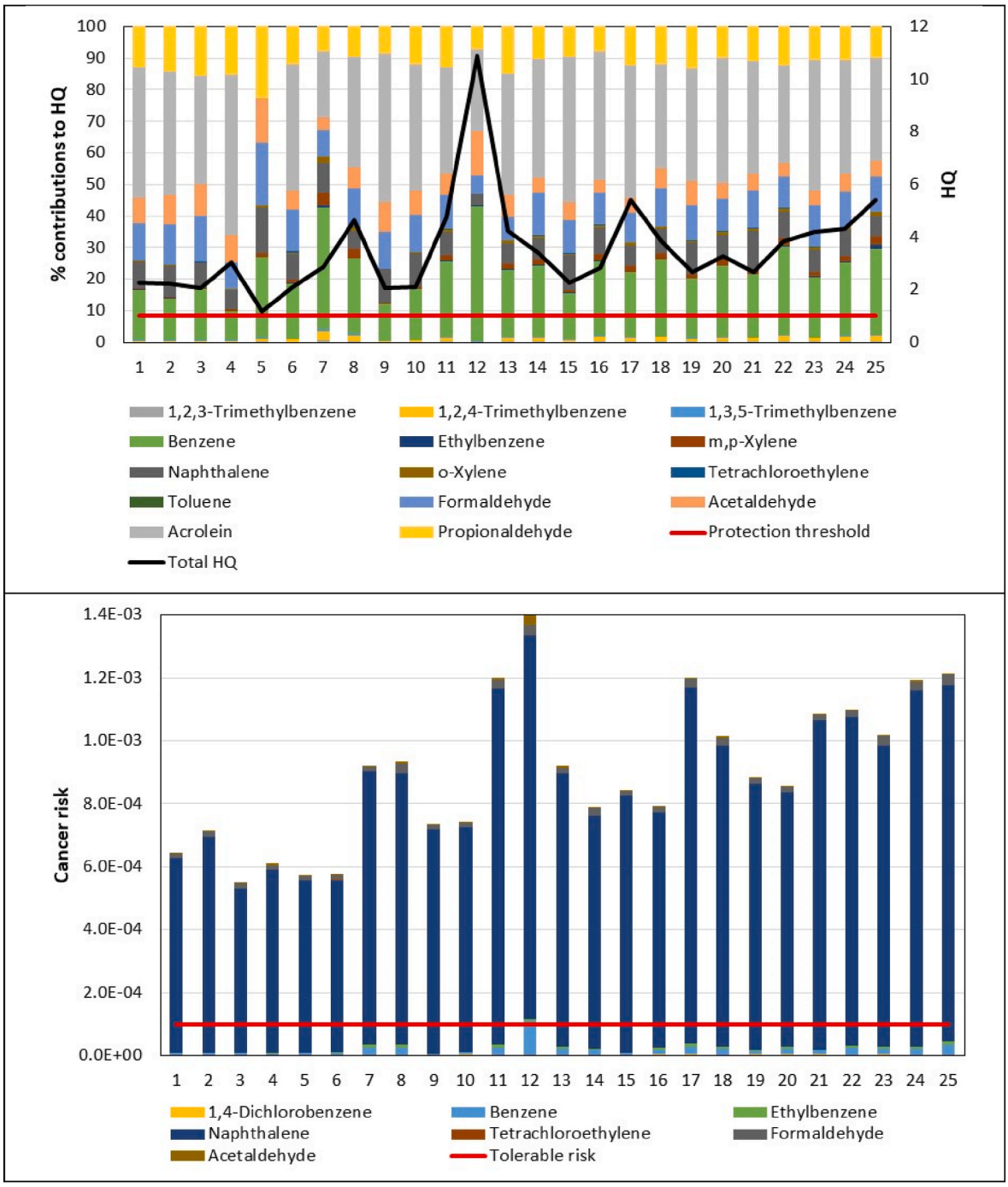

Fig. 6. Hazard quotients and life cancer risks associated with VOC inhalation at the 25 sampling sites in Greater Luanda.

with special concern for the landfill and the places most impacted by traffic (Fig. 6). On average, a lifetime cancer risk of 9×10^{-4} was obtained. This implies an estimated excess of 900 new cancer cases per million people over a lifetime of 70 years. The cancer risk was mainly due to naphthalene, which accounted, on average, for 94.6% of the total. For the CR to be below the acceptable level, the average concentration of naphthalene in the Luanda metropolitan area would have to be reduced to values below 1 ng m^{-3}. The moderate correlations of this compound with BTEX (r^2 = 0.4–0.7) indicate that, in addition to traffic, other emission sources, namely industrial activities, should be targeted by the implementation of measures.

HQ and cancer risk values in Luanda are within the range reported for the haze pollution season in urban atmospheres of China (Zhang et al., 2021). Given that there may be compounds in the atmosphere with potential health risks that have not been quantified, the values obtained should be taken as default estimates.

As shown in Table S4, benzene was the compound that presented the highest risk index. Their R values correspond to moderate risks in residential or urban background areas to high risks at the Mulenvos landfill and in places most impacted by traffic. Formaldehyde and acetaldehyde also deserve attention for their moderate to high risks.

4. Conclusions

This study reports the results of the first monitoring campaign for gaseous pollutant concentrations ever carried out at multiple points in

the Luanda metropolitan region. Excepting ozone, the levels of regulated pollutants were below the values recommended by the WHO. For most pollutants, the highest levels were observed at locations most impacted by traffic. The Mulenvos landfill, surrounded by high-density settlements and where many hundreds of people pick up trash every day, stood out for its high concentrations of various compounds. All hazard quotient values were in the range from 1 to 11, indicating moderate to high risk of developing non-cancer diseases. The cancer risks associated with the inhalation of VOCs exceeded the tolerable level. Since the cancer risk was mainly due to naphthalene, specific measures must be taken to reduce the levels of this pollutant. In general, the results point to traffic as the main emission source for many of the compounds monitored. Therefore, authorities should pay special attention to air quality improvement plans focused on the road sector. Given the legal void, Angola must adopt health-based air quality targets. Furthermore, regular monitoring of air quality should also be a goal of the authorities, as this allows the effectiveness of environmental policies and the effects of protective actions to be assessed.

As has long been observed in Europe, the atmospheric concentrations of ground-level ozone may represent a serious concern in Angola, not only because of its harmful repercussions on human health but also due to its damaging effects on vegetation, leading to reduced crop yields and forest growth, and loss of biodiversity. The counterintuitive phenomenon of higher levels in traffic locations should be the subject of an in-depth study in the future considering meteorological and synoptic conditions, scavenging processes, long-range transport and dispersal of precursors, vegetation phenology and asymmetries in land cover.

This study should be seen as the first screening of air quality in the metropolitan region of Luanda, and it needs to be complemented with additional measurements to evaluate seasonal patterns and variability of concentrations on shorter time scales.

CRediT authorship contribution statement

Célia A. Alves: Writing – original draft, Supervision, Project administration, Methodology, Investigation, Funding acquisition, Conceptualization. **Manuel J.S. Feliciano:** Writing – review & editing, Supervision, Resources, Investigation. **Carla Gama:** Writing – review & editing, Formal analysis. **Estela Vicente:** Writing – review & editing, Methodology. **Leonardo Furst:** Writing – review & editing, Methodology. **Anabela Leitão:** Writing – review & editing, Resources, Conceptualization.

Declaration of competing interest

The authors declare that they have no known competing financial interests or personal relationships that could have appeared to influence the work reported in this paper.

Data availability

Data will be made available on request.

Acknowledgements

The Portuguese Foundation for Science and Technology (FCT) is acknowledged for the PhD fellowship to L. Furst (SRFH/BD/08461/2020) and the CEEC contracts to C. Gama (2021.00732.CEECIND) and E. Vicente (DOI: 10.54499/2022.00399.CEECIND/CP1720/CT0012). The financial support to CESAM by FCT/MCTES (UIDP/50017/2020 + UIDB/50017/2020 + LA/P/0094/2020), through national funds, is also acknowledged. This work was developed within the project "Air Pollution in an African Megacity: Source Apportionment and Health Implications – APAM" (DOI: 10.54499/2022.04240.PTDC), financially supported by national funds (OE), through FCT/MCTES. The logistical support from Luanda Civil Protection Services (Laurindo Canjo), Ministry of Environment (Rebeca Chingala) and Luanda Provincial Government (Lúcia Duque, Nadine Guimarães and Artur Freitas) is deeply appreciated.

Appendix A. Supplementary data

Supplementary data to this article can be found online at https://doi.org/10.1016/j.envpol.2024.125015.

References

Adon, M., Galy-Lacaux, C., Yoboue, V., Delon, C., Lacaux, J.P., Castera, P., Gardrat, E., Pienaar, J., Al Ourabi, H., Laouali, D., Diop, B., Sigha-Nkamdjou, L., Akpo, A., Tathy, J.P., Lavenu, F., Mougin, E., 2010. Long term measurements of sulfur dioxide, nitrogen dioxide, ammonia, nitric acid and ozone in Africa using passive samplers. Atmos. Chem. Phys. 10, 7467–7487. https://doi.org/10.5194/acp-10-7467-2010.

Adon, M., Yobou, V., Galy-Lacaux, C., Liousse, C., Diop, B., Doumbia, E.H.T., Gardrat, E., Ndiaye, S.A., Jarnot, C., 2016. Measurements of NO_2, SO_2, NH_3, HNO_3 and O_3 in West african urban environments. Atmos. Environ. 135, 31–40. https://doi.org/10.1016/j.atmosenv.2016.03.050.

Alvarez, C.M., Hourcade, R., Lefebvre, B., Pilot, E., 2020. A scoping review on air quality monitoring, policy and health in West African cities. Int. J. Environ. Res. Publ. Health 17, 9151. https://doi.org/10.3390/ijerph17239151.

Alves, C.A., Candeias, C., Nunes, T.V., Tome, M.J.C., Vicente, E.D., Avila, P.F., Rocha, F., 2018. Passive monitoring of particulate matter and gaseous pollutants in Fogo Island, Cape Verde. Atmos. Res. 214, 250–262. https://doi.org/10.1016/j.atmosres.2018.08.002.

Atkinson, R., Arey, J., 2003. Atmospheric degradation of volatile organic compounds. Chem. Rev. 103, 4605–4638. https://doi.org/10.1021/cr0206420.

Bahino, J., Yoboué, V., Galy-Lacaux, C., Adon, M., Akpo, A., Keita, S., Liousse, C., Gardrat, E., Chiron, C., Ossohou, M., Gnamien, S., Djossou, J., 2018. A pilot study of gaseous pollutants' measurement (NO_2, SO_2, NH_3, HNO_3 and O_3) in Abidjan, Côte d'Ivoire: contribution to an overview of gaseous pollution in African cities. Atmos. Chem. Phys. 18, 5173–5198. https://doi.org/10.5194/acp-18-5173-2018.

Barletta, B., Meinardi, S., Simpson, I.J., Khwaja, H.A., Blake, D.R., Rowland, F.S., 2002. Mixing ratios of volatile organic compounds (VOCs) in the atmosphere of Karachi, Pakistan. Atmos. Environ. 36, 3429–3443. https://doi.org/10.1016/S1352-2310(02)00302-3.

Bauer, S.E., Im, U., Mezuman, K., Gao, C.Y., 2019. Desert dust, industrialization, and agricultural fires: health impacts of outdoor air pollution in Africa. J. Geophys. Res. Atmos. 124, 4104–4120. https://doi.org/10.1029/2018JD029336.

Berezina, E., Moiseenko, K., Skorokhod, A., Pankratova, N.V., Belikov, I., Belousov, V., Elansky, N.F., 2020. Impact of VOCs and NOx on ozone formation in Moscow. Atmosphere 11, 1262. https://doi.org/10.3390/atmos11111262.

Cachon, B., Ayi-Fanou, L., Cazier, F., Genevray, P., Adéoti, K., Dewaele, D., Debende, A., Aissi, F., Sanni, A., 2013. Analysis of gasoline used by motorbike-taxi drivers in Cotonou. Environ. Pollut. 2, 39–48. https://doi.org/10.5539/ep.v2n2p39.

Campos, P., Esteves, A., Leitão, A., Pires, J., 2021. Design of air quality monitoring network of Luanda, Angola: urban air pollution assessment. Atmos. Pollut. Res. 12, 101128. https://doi.org/10.1016/j.apr.2021.101128.

Chen, Y., Shi, Y., Ren, J., You, G., Zheng, X., Liang, Y., Simayi, M., Hao, Y., Xie, S., 2023. VOC species controlling O_3 formation in ambient air and their sources in Kaifeng, China. Environ. Sci. Pollut. Res. 30, 75439–75453. https://doi.org/10.1007/s11356-023-27595-w.

Cordell, R.J., Panchal, R., Bernard, E., Gatari, M., Waiguru, E., Ng'ang'a, M., Nyang'aya, J., Ogot, M., Wilde, M.J., Wyche, K.P., Abayomi, A.A., Alani, R., Monks, P.S., Hey, J.D.V., 2021. Volatile organic compound composition of urban air in Nairobi, Kenya and Lagos, Nigeria. Atmosphere 12, 1329. https://doi.org/10.3390/atmos12101329.

Delikhoona, M., Fazlzadeh, M., Sorooshian, A., Baghani, A.N., Golaki, M., Ashournejad, Q., Barkhordari, A., 2018. Characteristics and health effects of formaldehyde and acetaldehyde in an urban area in Iran. Environ. Pollut. 242, 938–951. https://doi.org/10.1016/j.envpol.2018.07.037.

Derwent, R.G., Jenkin, M.E., Utembe, S.R., Shallcross, D.E., Murrells, T.P., Passant, N.R., 2010. Secondary organic aerosol formation from a large number of reactive man-made organic compounds. Sci. Total Environ. 408, 3374–3381. https://doi.org/10.1016/j.scitotenv.2010.04.013.

El-Ghazi, A., El-Hassani, Y.A., Laziri, F., El-Jaafari, S., 2023. Evaluation of nitrogen dioxide, benzene, toluene, ethylbenzene and xylene concentrations in the urban environment of Meknes City, Morocco. Asian J. Adv. Agric. Res. 23. https://doi.org/10.9734/AJAAR/2023/v23i3463. Article no.AJAAR.107265.

EPA, 2014. Passive Samplers for Investigations of Air Quality: Method Description, Implementation, and Comparison to Alternative Sampling Methods. United States Environmental Protection Agency, Cincinnati, OH. EPA/600/R-14/434. Office of Research and Development, National Risk Management Research Laboratory.

Government of British Columbia, 2018. Standard operating procedure for the passive/diffusive method of air sample collection. Ministry of Environment and Climate Change Strategy. BC, Canada.

Greenstone, M., Fan, C.Q., 2018. Introducing the Air Quality Life Index. Twelve Facts about Particulate Air Pollution, Human Health, and Global Policy. Energy Policy Institute at the University of Chicago. https://aqli.epic.uchicago.edu/wp-content/uploads/2018/11/AQLI-Annual-Report-V13.pdf.

Guéniat, M., Harjono, M., Missbach, A., Viredaz, G.V., 2016. Dirty Diesel. How Swiss Traders Flood Africa with Toxic Fuels. A Public Eye Investigation. Public Eye, Lausanne, Switzerland. https://www.publiceye.ch/fileadmin/doc/Rohstoffe/2016_PublicEye_Dirty_Diesel_Report.pdf.

Guo, H., Zou, S.C., Tsai, W.Y., Chan, L.Y., Blake, D.R., 2011. Emission characteristics of nonmethane hydrocarbons from private cars and taxis at different driving speeds in Hong Kong. Atmos. Environ. 45, 2711–2721. https://doi.org/10.1016/j.atmosenv.2011.02.053.

Guo, S.J., Chen, M., He, X.L., Yang, W.W., Tan, J.H., 2014. Seasonal and diurnal characteristics of carbonyls in urban air in Qinzhou, China. Aerosol Air Qual. Res. 14, 1653–1664. https://doi.org/10.4209/aaqr.2013.12.0351.

Hou, S., Wang, Y., Duan, L., Xiu, G., 2024. Health risk assessment from exposure to ambient volatile organic compounds (VOCs) at a truck tire factory in the Yangtze River Delta, China. Atmosphere 15, 458. https://doi.org/10.3390/atmos15040458.

Hui, L., Liu, X., Tan, Q., Feng, M., An, J., Qu, Y., Zhang, Y., Jiang, M., 2018. Characteristics, source apportionment and contribution of VOCs to ozone formation in Wuhan, Central China. Atmos. Environ. 192, 55–71. https://doi.org/10.1016/j.atmosenv.2018.08.042.

Jaars, K., Vestenius, M., van Zyl, P.G., Beukes, J.P., Hellén, H., Vakkari, V., Venter, M., Josipovica, M., Hakola, H., 2018. Receptor modelling and risk assessment of volatile organic compounds measured at a regional background site in South Africa. Atmos. Environ. 172, 133–148. https://doi.org/10.1016/j.atmosenv.2017.10.047.

Josipovic, M., Annegarn, H.J., Kneen, M.A., Pienaar, J.J., Piketh, S.J., 2010. Concentrations, distributions and critical level exceedance assessment of SO_2, NO_2 and O_3 in South Africa. Environ. Monit. Assess. 171, 181–196. https://doi.org/10.1007/s10661-009-1270-5.

Kerbachi, R., Boughedaoui, M., Bounoua, L., Keddam, M., 2006. Ambient air pollution by aromatic hydrocarbons in Algiers. Atmos. Environ. 40, 3995–4003. https://doi.org/10.1016/j.atmosenv.2006.02.033.

Kim, S.J., Kwon, H.O., Lee, M.I., Seo, Y., Choi, S.D., 2019. Spatial and temporal variations of volatile organic compounds using passive air samplers in the multi-industrial city of Ulsan, Korea. Environ. Sci. Pollut. Res. 26, 5831–5841. https://doi.org/10.1007/s11356-018-4032-5.

Kirenga, B.J., Meng, Q., van Gemert, F., Aanyu-Tukamuhebwa, H., Chavannes, N., Katamba, A., Obai, G., van der Molen, T., Schwander, S., Mohsenin, V., 2015. The state of ambient air quality in two Ugandan cities: a pilot cross-sectional spatial assessment. Int. J. Environ. Res. Publ. Health 12, 8075–8091. https://doi.org/10.3390/ijerph120708075.

Leikauf, G.D., 2020. Formaldehyde and other saturated aldehydes. Chapter 16. In: Lippmann, M., Leikauf, G.D. (Eds.), Environmental Toxicants: Human Exposures and Their Health Effects, fourth ed. John Wiley & Sons Inc., Hoboken, NJ, USA https://doi.org/10.1002/9781119438922.ch16.

Li, Q., Su, G., Li, C., Liu, P., Zhao, X., Zhang, C., Sun, B., 2020. An investigation into the role of VOCs in SOA and ozone production in Beijing, China. Sci. Total Environ. 720, 137536. https://doi.org/10.1016/j.scitotenv.2020.137536.

Liu, T., Sun, J., Liu, B., Li, M., Deng, Y., Jing, W., Yang, J., 2022. Factors influencing O_3 concentration in traffic and urban environments: a case study of Guangzhou City. Int. J. Environ. Res. Publ. Health 19, 12961. https://doi.org/10.1002/10.3390/ijerph191912961.

LoPachin, R.M., Gavin, T., 2014. Molecular mechanisms of aldehyde toxicity: a chemical perspective. Chem. Res. Toxicol. 27, 1081–1091. https://doi.org/10.1021/tx5001046.

Lourens, A.S., Beukes, J.P., van Zyl, P.G., Fourie, G.D., Burger, J.W., Pienaar, J.J., Read, C.E., Jordaan, H.H., 2011. Spatial and temporal assessment of gaseous pollutants in the Highveld of South Africa. S. Afr. J. Sci. 107, 269. https://doi.org/10.4102/sajs.v107i1/2.269.

Lü, L., Cai, Q.Y., Wen, S., Chi, Y., Guo, S., Sheng, G., Fu, J., 2010. Seasonal and diurnal variations of carbonyl compounds in the urban atmosphere of Guangzhou. China. Sci. Total Environ. 408, 3523–3529. https://doi.org/10.1016/j.scitotenv.2010.05.013.

Makoni, M., 2020. Air pollution in Africa. Lancet Respir. Med. 8, E60–E61. https://doi.org/10.1016/S2213-2600(20)30275-7.

Marchand, C., Bulliot, B., Le Calve, S., Mirabel, Ph., 2006. Aldehyde measurements in indoor environments in Strasbourg (France). Atmos. Environ. 40, 1336–1345. https://doi.org/10.1016/j.atmosenv.2005.10.027.

Matysik, S., Ramadan, A.B., Schlink, U., 2010. Spatial and temporal variation of outdoor and indoor exposure of volatile organic compounds in Greater Cairo. Atmos. Pollut. Res. 1, 94–101. https://doi.org/10.5094/apr.2010.012.

Monod, M., Sive, B.C., Avino, P., Chen, T., Blake, D.R., Rowland, F.S., 2001. Monoaromatic compounds in ambient air of various cities: a focus on correlations between the xylenes and ethylbenzene. Atmos. Environ. 35, 135–149.

Moodley, K.G., Singh, S., Govender, S., 2011. Passive monitoring of nitrogen dioxide in urban air: a case study of Durban metropolis, South Africa. J. Environ. Manage. 92, 2145–2150. https://doi.org/10.1016/j.jenvman.2011.03.040.

Muñoz Sabater, J., 2019. ERA5-Land hourly data from 1950 to present. Copernicus Climate Change Service (C3S) Climate Data Store (CDS). https://doi.org/10.24381/cds.e2161bac. (Accessed 17 July 2024).

Nair, A.T., Senthilnathan, J., Nagendra, S.M.S., 2019. Emerging perspectives on VOC emissions from landfill sites: impact on tropospheric chemistry and local air quality. Process Saf. Environ. Prot. 121, 143–154. https://doi.org/10.1016/j.psep.2018.10.026.

Nana, B., Sanogo, O., Savadogo, P.W., Daho, T., Bouda, M., Koulidiati, J., 2012. Air quality in urban centers: case study of Ouagadougou, Burkina Faso. FUTY J. Environ. 7 (1), 1–17. https://doi.org/10.4314/fje.v7i1.1.

Ngoasheng, M., Beukes, J.P., van Zyl, P.G., Swartz, J.S., Loate, V., Krisjan, P., Mpambani, S., Kulmala, M., Vakkari, V., Laakso, L., 2021. Assessing SO_2, NO_2 and O_3 in rural areas of the North West West Province. Clean Air J. 31. https://doi.org/10.17159/caj/2021/31/1.9087.

Ouabourrane, Z., El Abassi, M., El Haddaj, H., Bazzi, L., Hanoune, B., El Maimouni, L., 2017. BTX and carbonyl compounds in the roadside environments of Inezgane Ait Melloul (southwestern Morocco). J. Mat. Environ. Sci. 8, 611–621.

Pan, Q., Liu, Q.Y., Zheng, J., Li, Y.H., Xiang, S., Sun, X.J., He, X.S., 2023. Volatile and semi-volatile organic compounds in landfill gas: composition characteristics and health risks. Environ. Int. 174, 107886. https://doi.org/10.1016/j.envint.2023.107886.

Rees, N., Wickham, A., Choi, Y., 2019. Silent Suffocation in Africa: Air Pollution Is a Growing Menace. Hitting the Poorest Children Hardest. UNICEF, New York. https://www.unicef.org/reports/silent-suffocation-in-africa-air-pollution-2019.

Sekar, A., Varghese, G.K., Varma, M.K.R., 2019. Analysis of benzene air quality standards, monitoring methods and concentrations in indoor and outdoor environment. Heliyon 5, e02918. https://doi.org/10.1016/j.heliyon.2019.e02918.

Swartz, J.S., Van Zyl, P.G., Beukes, J.P., Labuschagne, C., Brunke, E.G., Portafaix, T., Galy-Lacaux, C., Pienaar, J.J., 2020. Twenty-one years of passive sampling monitoring of SO_2, NO_2 and O_3 at the Cape Point GAW station, South Africa. Atmos. Environ. 222, 117128. https://doi.org/10.1016/j.atmosenv.2019.117128.

Thabethe, N.D.J., Engelbrecht, J.C., Wright, C.Y., Oosthuizen, M.A., 2014. Human health risks posed by exposure to PM_{10} for four life stages in a low socioeconomic community in South Africa. Pan Afr. Med. J. 18, 206. https://doi.org/10.11604/pamj.2014.18.206.3393.

Tan, J.H., Guo, S.J., Ma, Y.L., Yang, F.M., He, K.B., Yu, Y.C., Wang, J.W., Shi, Z.B., Chen, G.C., 2012. Non-methane hydrocarbons and their ozone formation potentials in Foshan, China. Aerosol Air Qual. Res. 12, 387–398. https://doi.org/10.4209/aaqr.2011.08.0127.

Tian, M., Xia, P., Yan, L., Gou, X., Giesy, J.P., Dai, J., Yu, H., Zhang, X., 2022. Toxicological mechanism of individual susceptibility to formaldehyde-induced respiratory effects. Environ. Sci. Technol. 56, 6511–6524. https://doi.org/10.1021/acs.est.1c07945.

Tsiligiannis, E., Hammes, J., Salvador, C.M., Mentel, T.F., Hallquist, M., 2019. Effect of NOx on 1,3,5-trimethylbenzene (TMB) oxidation product distribution and particle formation. Atmos. Chem. Phys. 19, 15073–15086. https://doi.org/10.5194/acp-19-15073-2019.

Venecek, M.A., Carter, W.P.L., Kleeman, M.J., 2018. Updating the SAPRC maximum incremental reactivity (MIR) scale for the United States from 1988 to 2010. J. Air Waste Manag. Assoc. 68, 1301–1316. https://doi.org/10.1080/10962247.2018.1498410.

Wang, J., Chen, S., Qiu, X., Niu, W., Li, O., Zhu, C., Zhang, X., Yang, X., Zhang, G., 2022. Pollution characteristics of atmospheric carbonyl compounds in a large city of Northern China. J. Chem. 2022, 3292598. https://doi.org/10.1155/2022/3292598.

WHO, 2016. Ambient Air Pollution: a Global Assessment of Exposure and Burden of Disease. WHO, Geneva, Switzerland. https://apps.who.int/iris/handle/10665/250141.

WHO, 2018. Air Pollution and Child Health: Prescribing Clean Air. World Health Organization, Geneva, Switzerland. WHO/CED/PHE/18.01. https://www.who.int/publications/i/item/WHO-CED-PHE-18-01.

Zhang, D., He, B., Yuan, M., Yu, S., Yin, S., Zhang, R., 2021. Characteristics, sources and health risks assessment of VOCs in Zhengzhou, China during haze pollution season. J. Environ. Sci. 108, 44–57. https://doi.org/10.1016/j.jes.2021.01.035.

Zhang, Y., Wang, X., Barletta, B., Simpson, I.J., Blake, D.R., Fu, X., Zhang, Z., He, Q., Liu, T., Zhao, X., Ding, X., 2013. Source attributions of hazardous aromatic hydrocarbons in urban, suburban and rural areas in the Pearl River Delta (PRD) region. J. Hazard Mater. 250–251, 403–411. https://doi.org/10.1016/j.jhazmat.2013.02.023.

Zhang, Z., Zhang, Y., Wang, X., Lü, S., Huang, Z., Huang, X., Yang, W., Wang, Y., Zhang, Q., 2016. Spatiotemporal patterns and source implications of aromatic hydrocarbons at six rural sites across China's developed coastal regions. J. Geophys. Res. Atmos. 121, 6669–6687. https://doi.org/10.1002/2016JD025115.